Active Airframe Vibration Control Study Using a Small-Scale Model for Lift-Offset Compound Helicopter

Shin-Won Bang[1] · Sung-Boo Hong[2] · Yu-Been Lee[1] · Hyun-Cheol Shin[1] · Byeong-Hyeon Park[1] · Jae-Sang Park[1]

Abstract

The present study using active vibration control system (AVCS) attempts to actively reduce the airframe vibration responses of a lift-offset compound helicopter at 250 knots. An 11% scaled airframe structure of the Sikorsky X2 Technology Demonstrator (TD) is used for the AVCS test and simulation and this small-scale airframe model is designed and manufactured based on the one-dimensional (1D) stick structure. The present AVCS comprises two force generators for producing vibration cancellation forces, two accelerometers to measure 4P vertical vibration responses at the pilot and copilot seats, and the filtered-x least mean square (Fx-LMS) algorithm as a closed-loop feedback controller. MATLAB Simulink is used to construct the AVCS framework for both tests and simulations. MSC.NASTRAN is applied to the dynamic design of a small-scale airframe structure and to predict of its airframe vibration responses in a simulation study. The dSPACE MicrolabBox equipment is used for the AVCS test. When the AVCS is applied to the present X2TD scaled airframe model, the 4P vertical vibration responses in the test are reduced by 68.57% and 60.24% compared to the baseline without AVCS at the pilot and copilot seats, respectively, whereas they are reduced by 70.89% and 64.11%, respectively, in the simulation. Finally, the vertical vibration reduction rates between the AVCS test and simulation are similar, and it is investigated that the vibration reduction performance is good in both the AVCS test and simulation.

Keywords Lift-offset compound helicopter · X2 technology demonstrator · Small-scale airframe model · Active vibration control system

1 Introduction

A helicopter is an aircraft that has distinct characteristics such as hovering and vertical take-off/landing (VTOL) flights. However, the slow forward flight speed (approximately 150–170 knots) of conventional helicopters is challenge. Therefore, compound or convertible helicopters have recently been developed to solve this drawback of low-speed flight while maintaining hover and VTOL flight capabilities. For a compound helicopter using rotors, wings, and auxiliary propulsions, the lift-offset compound helicopter has received considerable attention because it exhibits high-speed flight capability and can maintain the hover performance of conventional helicopters. A lift-offset compound helicopter using a lift-offset coaxial rotor (or rigid coaxial rotor) produces most of the lift forces on each advancing side. Therefore, the retreating blades are off-loaded and dynamic stall on the retreating side is not experienced. Furthermore, the lift-offset rotor can be slowed down; thus, high-speed flight is possible when auxiliary propulsions are used [1–3]. The X2 technology demonstrator (TD) (Fig. 1a), developed by Sikorsky, is a modern lift-offset compound helicopter based on XH-59A (Fig. 1b), and is the baseline model for advanced lift-offset compound helicopters such as the S-97 Raider (Fig. 1c), and SB > 1 Defiant (Fig. 1d).

However, the lift-offset rotor has very rigid blades; thus, lift-offset compound helicopters experience a high level of N_b/rev vibration in high-speed flights compared with conventional helicopters [1], where N_b denotes the number of blades for a rotor and 1/rev (or 1P) is the non-dimensional rotor rotational speed. In high-speed flight conditions, significant

✉ Jae-Sang Park
aerotor@cnu.ac.kr

[1] Department of Aerospace Engineering, Chungnam National University, Daejeon 34134, Republic of Korea

[2] Mechanical Design Team, Fundamental Technology Research Center, Hanwha Systems, Yongin 17121, Republic of Korea

(a) X2 Technology Demonstrator

(b) XH-59A

(c) S-97 Raider

(d) SB>1 Defiant

Fig. 1 Various lift-offset compound helicopters

Table 1 General properties of X2TD lift-offset compound helicopter

Property	Value
Gross weight, GW	5955 lb
Fuselage length	29.1 ft
Number of rotors	2
Number of blades per rotor, N_b	4
Rotor solidity (total), σ	0.1441
Rotor radius, R	13.2 ft
Nominal tip speed, V_{tip}	620.45 ft/sec
Maximum level flight speed	250 knots
Rotor vertical separation	1.5 ft
Advancing blade tip Mach number	0.9
Nominal rotor speed (at hover)	448.5 RPM
Rotor speed at speed of 250 knots	394.7 RPM
Pusher propeller radius	3.335 ft
Horizontal tail area	34 ft^2
Vertical tail area	15.4 ft^2

vibrations cause negative effects such as limited maximum flight speed, degradation of the structural integrity, increase in fatigue of the mechanical components, passenger discomfort, increase in life-cycle cost, and mechanical malfunction [4]. Therefore, reducing helicopter vibrations by applying appropriate vibration control techniques is important.

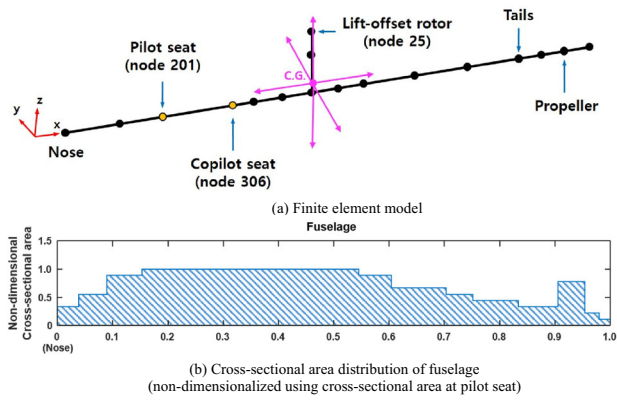For lift-offset compound helicopters, the rotor speed is appropriately reduced during high-speed flights. Therefore, active vibration control techniques, which can be used in a wider frequency range, are more appropriate than passive vibration control techniques, which are effective in a limited frequency range [4]. The active vibration control system (AVCS), which has been applied to conventional helicopters (S-76D, AW139, and UH60M) and lift-offset compound helicopters (X2TD, S-97 Raider, and SB > 1 Defiant), demonstrates excellent airframe vibration reduction performance. The AVCS comprises force generators, accelerometers, and a closed-loop controller. The AVCS suppresses airframe vibration by generating vibration cancellation signals that sum to zero with the airframe vibration responses excited from the rotor [3–7].

In the design stage of rotorcraft, experimentally applying AVCS to a full-scale aircraft is difficult; however, AVCS simulation is available for both full- and small-scale models. Therefore, when the experimental work using AVCS is considered in the preliminary design, the small-scale airframe model is more appropriate than the full-scale model. Small-scale airframe models of conventional helicopters (AH-1G [8],), tiltrotor aircraft (V-22 [9],), and the conceptual lift-offset unmanned compound helicopter [10] using a lift-offset coaxial rotor, wings, and propellers were considered for experimental work using AVCS. However, there have been no published experimental works for active airframe vibration controls using a small-scaled model for the actual lift-offset compound helicopters, which succeeded in flights.

Therefore, in this study, it is conducted that tests and simulations using AVCS for a small-scale airframe model for X2TD in high-speed flights. X2TD is a good model for this study because there are available data in the public domain

(a) Finite element model

(b) Cross-sectional area distribution of fuselage
(non-dimensionalized using cross-sectional area at pilot seat)

Fig. 2 Full-scale airframe stick model of X2TD in free–free boundary conditions

Table 2 Target natural frequencies of X2TD airframe structure

Mode	Frequency [Hz]
1st fuselage lateral bending mode	7.5–8.5
1st fuselage vertical bending mode	11.5–13.0
2nd fuselage lateral bending mode	21.0–23.5
2nd fuselage vertical bending mode	31.5–35.5

Table 3 Natural frequencies of full-scale airframe model

| Mode | Natural frequency [Hz] | | Error [%] |
	Modal analysis model (free–free B.C.)	Ground vibration test model	
1st lateral bending mode	7.612	7.620	0.105
1st vertical bending mode	11.650	11.712	0.532
2nd lateral bending mode	22.862	22.856	− 0.026
2nd vertical bending mode	33.034	34.233	3.630

for X2TD, as compared to the S-97 Raider and SB > 1 Defiant. The X2TD demonstrated excellent airframe vibration reduction by applying the AVCS through flight tests and simulation studies [3]. A full-scale one-dimensional (1D) stick (elastic-line) model in free–free boundary conditions for the X2TD airframe structure is represented by MSC.NASTRAN (a finite-element analysis software), and an 11% dynamically scaled model using 1D bar elements is constructed based on the full-scale model. A small-scale ground vibration test (GVT) model, along with steel cables and springs is designed and manufactured. At a flight speed of 250 knots, the 4P airframe vibration responses at the pilot and copilot seats are calculated using the full- and small-scale GVT models, measured experimentally for the manufactured small-scale GVT model, and compared to each other. In both the AVCS test and simulation, MATLAB Simulink is applied using the Fx-LMS algorithm [11]. The dSPACE ControlDesk, MicrolabBox, and MATLAB Simulink are used for the AVCS test using a small-scale X2TD airframe model. The 4P airframe vibration responses reduced by AVCS in the present test and simulation are compared, and the vibration reduction performance using AVCS is evaluated. Although the existing active vibration control technique, i.e., AVCS, is applied for this study, the comprehensive and practical work is conducted from the airframe structural design to the AVCS simulations and tests for active vibration reductions of the X2TD small-scaled airframe model.

2 Methods

2.1 Full-Scale Airframe Structural Dynamics Model

X2TD is a 6,000-lb class lift-offset compound helicopter developed by Sikorsky to realize the high-speed flight of a rotorcraft. In September 2010, a maximum speed of 250 knots was recorded during the level flight. The lift-offset rotor

of X2TD has four blades each of the upper and lower rotors; thus, the 4P frequency is the most important for X2TD vibration problems. Table 1 summarizes the general properties of the X2TD [3]. For the 4P airframe vibration response analysis at 250 knots, a full-scale airframe structural dynamics model is constructed using MSC.NASTRAN. As shown in Fig. 2a, the one-dimensional (1D) stick airframe structure using 36 elastic beam elements (CBARs) is remodeled based on previous work [12]. The 1D stick airframe model can represent similar modal characteristics and dynamic responses as those using the 3D airframe model, although a lower degree of freedoms is used for the 1D stick model. Hence, the 1D stick model is often used to predict the rotorcraft airframe vibration responses [13–15]. For full-scale stick modeling, the 3D drawings in reference [3] are used to model the geometric configuration. However, unlike the authors' previous work [12], the horizontal and vertical tails are not considered because the present study does not focus on them. The weight data for the X2TD airframe components are assumed by applying the well-known Mach scaling law to NASA's conceptual design results for the lift-offset compound helicopter [16], which has a configuration similar to that of X2TD. These weight values of airframe components are inputted to the stick model, using concentrated mass elements (CONM2) while considering that the gross weight
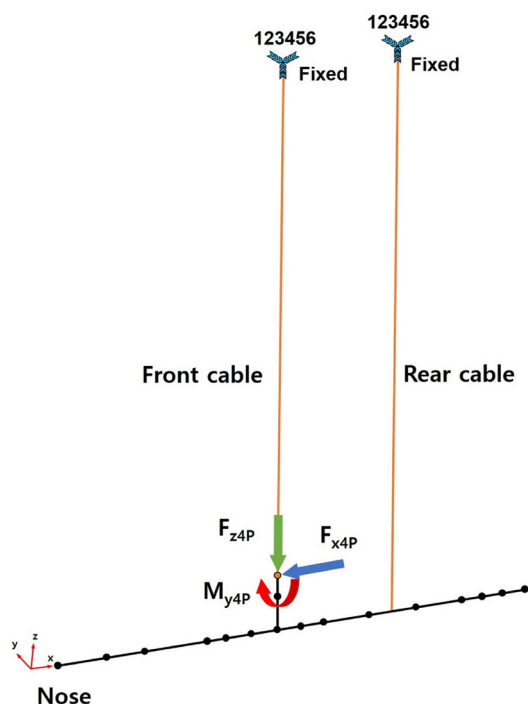
Fig. 3 Full-scale ground vibration test model of X2TD

is matched and the aircraft's center of gravity is located near the rotor axis. As previously described, the horizontal and vertical tails are not modeled, but only their weights are considered. Subsequently, the cross-sectional dimensions (Fig. 2b) and elastic material properties of the beam elements for this stick airframe model are designed for the full-scale stick model to have dynamic similarity with the actual X2TD airframe structure. The natural frequencies of the stick airframe model in the lower four fuselage bending modes are designed to satisfy the target natural frequencies of the X2TD airframe structure, as listed in Table 2. As the natural frequencies of the actual X2TD airframe are not provided in the public domain, the target natural frequencies of the airframe structure are assumed using the following procedures. First, the first lateral mode frequency can be estimated from the initial fuselage design results obtained by Sikorsky [3]. Second, the other three bending mode frequencies of the X2TD fuselage can be derived using its airframe configuration and the formula for the natural frequencies of the engineering beam model in free–free boundary conditions. As shown in Table 3, the modal analysis results for the present full-scale stick airframe model in free–free boundary conditions satisfy the target natural frequencies.

A ground vibration test (GVT) model (Fig. 3) is used to predict the 4P airframe vibration responses when 4P rotor hub vibratory loads are applied to the airframe [7, 17]. The GVT model is constructed by adding two bungee cables to the previous full-scale airframe stick model used for the

modal analysis. The lengths and material properties of the two bungee cables are determined such that the GVT model shows six rigid body modes in flight and has natural frequencies similar to those of the modal analysis model in free–free boundary conditions. The natural frequencies of the present GVT model are calculated by frequency response analysis with sinusoidal excitation using the 4P frequency in the vertical or lateral direction. The natural frequencies predicted by the frequency response analysis for the GVT model are compared well with those from the modal analysis, as summarized in Table 3 because the relative error between the two results is within 4%. Therefore, the GVT model for the full-scale airframe is believed to be appropriate for predicting the 4P airframe vibration responses of the X2TD in flight.

2.2 Small-Scale Airframe Structural Dynamics Model

The 11% dynamically scaled stick model (length: 1 m; weight: 5.66 kg) to the X2TD airframe is designed and manufactured for the AVCS test at a small laboratory in the university. Aluminum is selected as the structural material because it is easily manufactured. The cross-sectional dimensions and lengths of multiple blocks in Fig. 4 are determined such that the natural frequencies of the small-scale model in free–free boundary conditions predicted by the normal mode analysis are similar to those of the full-scale normal mode analysis model in the previous section. For this small-scale model, two different small-scale models are constructed using 1D beam elements (37 CBAR elements, Fig. 4a) and 3D solid elements (7622 CTETRA elements, Fig. 4b). As shown in Table 4 and Fig. 5, both normal mode analysis results for the two small-scale models match well with those of the full-scale airframe stick model.

Using the same method as the full-scale GVT model described in Sect. 2.1, the small-scale GVT model is constructed using the 1D stick model, as shown in Fig. 6. Steel cables and springs are added to the above-described small-scale airframe model to simulate the small-scale GVT model. The number of cables, their lengths and the number of springs are designed such that the natural frequencies of the small-scale GVT model are similar to those of the small-scale model using 3D elements in free–free boundary conditions and the small-scale GVT model has six rigid body modes. Table 5 summarizes the natural frequencies of the small-scale GVT model calculated using frequency response analysis. As shown in the table, the natural frequencies of the small-scale GVT model are compared excellently with the normal mode analysis results of the small-scale model using 3D elements. A small-scale GVT model is manufactured based on the previously discussed design results (Fig. 7). A modal test using an impact hammer is conducted to measure the natural frequencies (Fig. 8). The impact hammer excites the GVT model in the vertical or lateral direction, and seven single-axis

Fig. 4 11% dynamically scaled model of X2TD in free–free boundary conditions

(a) 1D element model

(b) 3D element model
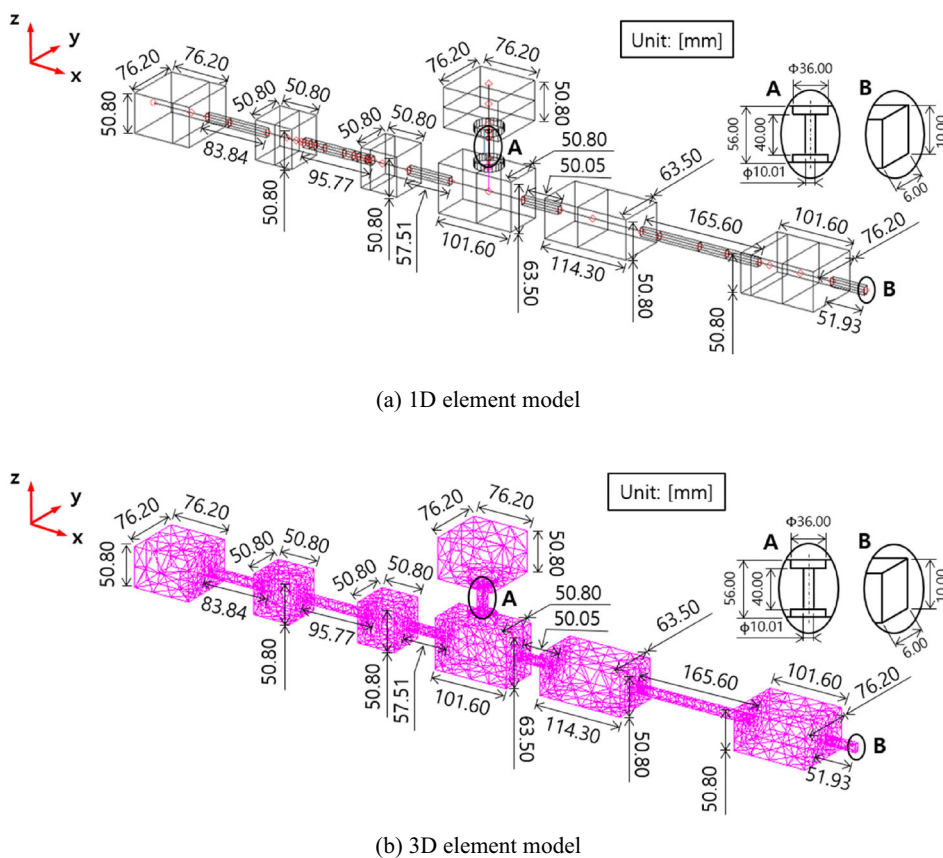
Table 4 Comparison of airframe natural frequencies between full-scale model and two different small-scale models

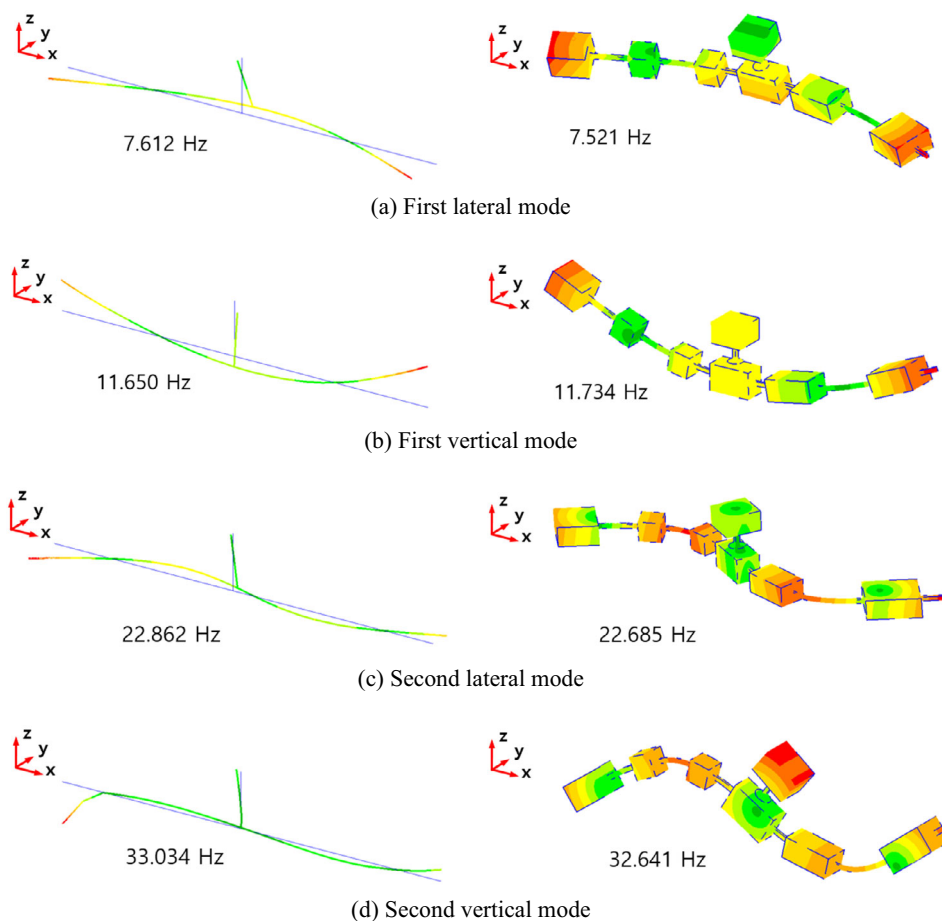| Mode	Natural frequency [Hz]		
	Full-scale model[1] (free–free B.C.)	Small-scale model (free–free B.C.)	
		1D elements[2] (difference[4])	3D elements[3] (difference[5])
1st lateral bending mode	7.612	7.799 (− 2.457%)	7.521 (− 1.195%)
1st vertical bending mode	11.650	11.989 (2.910%)	11.734 (0.721%)
2nd lateral bending mode	22.862	23.372 (2.231%)	22.685 (− 0.774%)
2nd vertical bending mode	33.034	32.820 (− 0.648%)	32.641 (− 1.190%)

[4]Difference between [1] and [2]
[5]Difference between [1] and [3]

accelerometers (Table 6) are located while avoiding the nodes in the mode shapes from the normal mode analysis using 3D elements. Table 5 compares the predicted and measured natural frequencies of the small-scale model with those of the full-scale model in free–free boundary conditions. As shown in the table, the modal test results have reasonable errors (less than 9%) against the natural frequencies of the full-scale

model predicted by the normal mode analysis. The Modal Assurance Criteria (MAC) in lower two bending modes are calculated to compare and evaluate the corresponding mode shapes of the small-scaled models in the finite-element analysis using 1D elements and modal test. As shown in Table 7 and Fig. 9, since the diagonal values in MAC are nearly 0.9 or higher, based on the reference [18], it is believed that

Fig. 5 Mode shapes of airframe stick model for X2TD. (Left: 1D full-scale model and right: 11% scaled model using 3D elements)

7.612 Hz   7.521 Hz

(a) First lateral mode

11.650 Hz   11.734 Hz

(b) First vertical mode

22.862 Hz   22.685 Hz

(c) Second lateral mode

33.034 Hz   32.641 Hz

(d) Second vertical mode

two sets of mode shapes obtained from the analysis and test are compared reasonably well for the small-scale airframe model. Therefore, the present small-scale GVT structure is appropriate for use in the AVCS test for the X2TD airframe.

2.3 AVCS for Airframe Vibration Reduction

The AVCS actively reduces the airframe vibration responses by minimizing the error signal, which is defined as the sum of the airframe vibration responses caused by the rotor hub vibratory loads and vibration cancellation responses generated from the force generator. The AVCS comprises sensors (① in Fig. 10), actuators (or force generators, ② in Fig. 10), and a closed-feedback controller (③ in Fig. 10). In this study, accelerometers are used to measure the airframe vibration responses, and the filtered-x least mean square (Fx-LMS) algorithm [11], which is an adaptive control algorithm, calculates the vibration cancellation signal with the same magnitude but antiphase (or in the opposite direction) to the airframe vibration response. A counter-rotating force generator (CRFG) and linear force generator are used in the AVCS simulation and test as force generators, respectively. As shown in Fig. 11, a CRFG generates a linear force as

the vibration cancellation force by the sum of two centrifugal forces of rotating disks [4]. The detailed properties of a CRFG in the present AVCS simulation using a full-scale airframe model are given in the reference [17]. Figure 12 shows a schematic diagram of the Fx-LMS algorithm. The reference input signal ($x(n)$) is the phase of the 4P signal of the rotor, and the disturbance path ($H(i\omega)$) is a transfer function model of the 4P airframe vibration responses caused by the rotor hub vibratory loads, where n represents the time step and ω is the 4P frequency. The forward path ($C(i\omega)$) represents the dynamic characteristics of the 4P vibration cancellation responses from the force generators, and is a mathematical transfer function model of the actual forward path ($C^*(i\omega)$). The control input signal ($u(n)$) is calculated using the LMS update equation [11] to minimize the error signal ($e(n)$, Eq. (1)) measured using the accelerometers:

$$e(n) = \hat{y}(n) + y(n) = C^*(i\omega)u(n) + y(n). \quad (1)$$

When the cost function J to minimize the error signal ($e(n)$) is defined by Eq. (2), the control input signal ($u(n)$) is updated using Eq. (3) with the gradient descending method
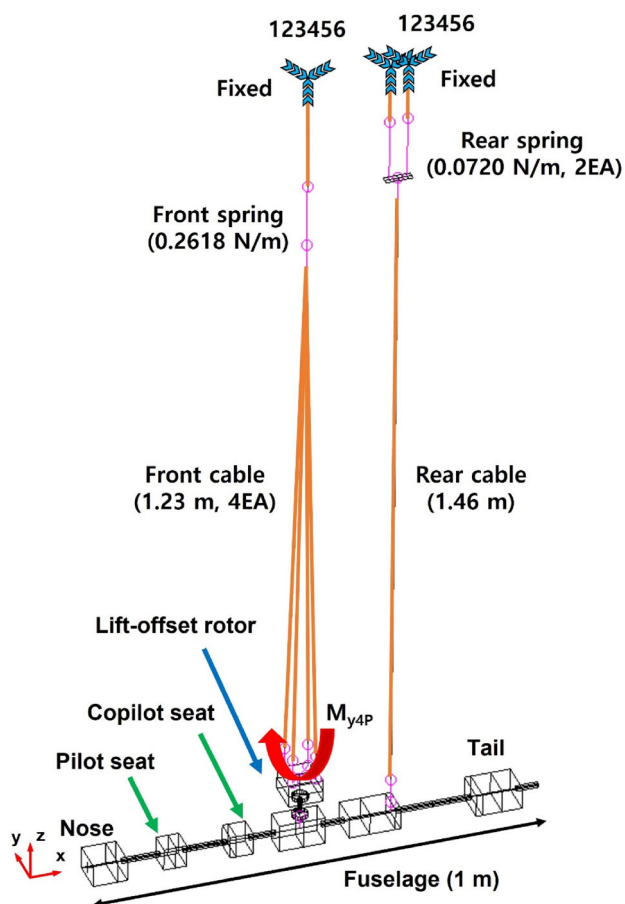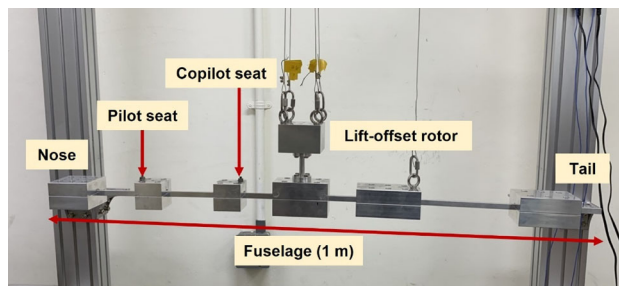
Fig. 6 Small-scale ground vibration test model of X2TD

Fig. 7 Manufactured small-scale ground vibration test model of X2TD

for every time step. As μ is a parameter that affects the convergence of the control input signal ($u(n)$) and the stability of the controller, its value should be appropriately selected [19]:

$$J = e^H(n)e(n), \tag{2}$$

$$u(n+1) = u(n) - \frac{1}{2}\mu\left(\frac{\partial J(n)}{\partial u(n)}\right). \tag{3}$$

The transfer function models in the AVCS are assumed to be linear time-invariant (LTI) systems, and they are obtained from the system identification using measured or calculated output values (vibration responses) for the given input values. The disturbance path ($H(i\omega)$) uses the 4P airframe vibration responses ($y(n)$) obtained when rotor hub vibratory loads are applied. The coefficients of the harmonic functions for the 4P airframe vibration response ($y(n)$), A_H, and B_H, are obtained using Eq. (4) with the MATLAB curve fitting tool. In this equation, the reference theta ($\theta(n)$) is the phase angle of the rotor hub vibratory loads at time step n and f represents the

Table 5 Dynamic similarity for small-scale ground vibration test model

Mode	Natural frequency [Hz]			
	Full-scale model[1] (free–free B.C.)	Small-scale model		
		3D elements (free–free B.C.)	Ground vibration test model using 1D elements	
			Freq. response analysis[2] (difference[4])	Modal test[3] (difference[5])
1st lateral bending mode	7.612	7.521	7.671 (0.775%)	8.250 (8.382%)
1st vertical bending mode	11.650	11.734	12.051 (3.442%)	11.000 (− 5.579%)
2nd lateral bending mode	22.862	22.685	23.360 (2.178%)	20.880 (− 8.669%)
2nd vertical bending mode	33.034	32.641	31.681 (− 4.096%)	31.130 (− 5.764%)

[4]Difference between [1] and [2]
[5]Difference between [1] and [3]
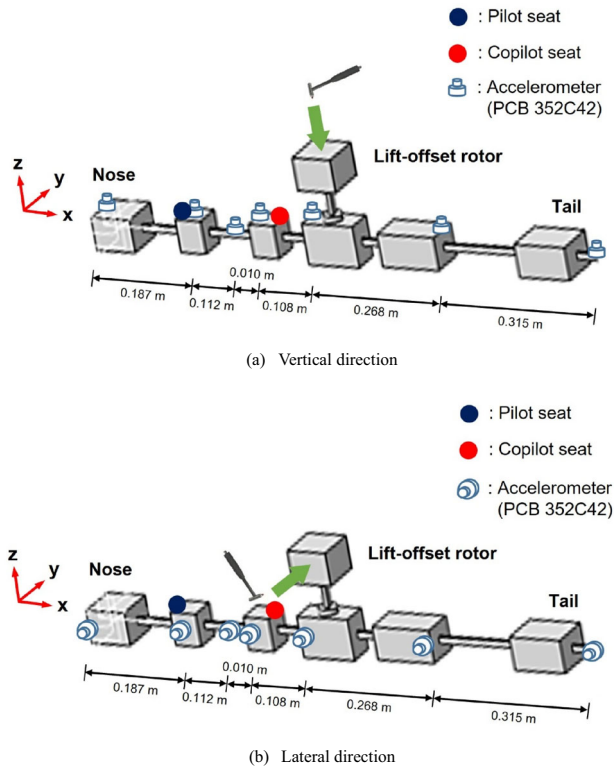
(a) Vertical direction

(b) Lateral direction

Fig. 8 Locations of accelerometers and excitation for modal test

Table 6 General properties of accelerometer

Parameter	Value
PCB 352C42	
Sensitivity (10%)	3.109 mV/ft/s^2
Broadband resolution	0.016 ft/s^2 rms (1 to 10,000 Hz)
Measurement range	$\pm$ 1,611 ft/s^2 pk
Frequency range ($\pm$ 5%)	1 to 9,000 Hz
Weight	0.006 lb
Height	0.382 in

N_b/revfrequency:

$$y(n) = A_H \cos \theta(n) + B_H \sin \theta(n), \tag{4}$$

where $\theta(n) = (2\pi f) \times t(n)$.

System identification for the actual forward path ($C^*(i\omega)$) is conducted using the control input signal ($u(n)$) and the airframe vibration response ($\hat{y}(n)$) by the vibration cancellation force, as given in Eq. (5):

$$\hat{y}(n) = C^*(i\omega)u(n)$$

$$= (A_{C^*} - i B_{C^*})(A \cos \theta(n) + B \sin \theta(n))$$
$$= A[A_{C^*} \cos \theta(n) + B_{C^*} \sin \theta(n)]$$
$$\quad + B[A_{C^*} \sin \theta(n) - B_{C^*} \cos \theta(n)]$$
$$= A_2 \cos \theta(n) + B_2 \sin \theta(n), \tag{5}$$

where $A_{C^*} = \frac{AA_2 + BB_2}{A^2 + B^2}$ and $B_{C^*} = \frac{AB_2 - BA_2}{A^2 + B^2}$.

2.4 AVCS Test Techniques

2.4.1 Experimental Setup

In this work, based on the author's previous works [10], as the three components of 4P hub vibratory loads (F_{x4P}, F_{z4P}, and M_{y4P}) cause airframe vibration [1], only the axial and vertical airframe vibration responses are considered. However, exciting the small-scale airframe model in the axial direction in the present AVCS test is not easy; thus, only vertical airframe vibration responses are used. Among the three 4P rotor hub vibratory load components, the 4P hub pitch moment (M_{y4P}), which has the greatest effect on the airframe vibration responses, is only used for the present AVCS test and simulation for the small-scale model [20]. Linear force generators are used to produce the 4P hub pitch moment and vibration cancellation forces in the AVCS test, and they are hung with steel cables and tensile springs so that their weights have no influence on the dynamic characteristics of the small-scale airframe model. A linear force generator (K2004E01 SmartShaker, ① in Fig. 13) produces a harmonic linear force in the vertical direction, which is applied to the tip of a moment arm with high rigidity. Therefore, a hub pitch moment can be generated using this linear force. However, the magnitude of the linear force generator for the 4P hub pitch moment is fixed as 75% of the force generator's maximum peak-to-peak force (31 N) in the experimental work so that the 4P airframe vibration responses at the specified locations (pilot and copilot seats) of the small-scale model are similar to those of the full-scale GVT model (Fig. 14). Two linear force generators (K2004E01 SmartShaker, ② in Fig. 13) for vibration cancellation forces are located at different positions for multi-input–multi-output (MIMO) model. The 4P vibration cancellation forces are limited to 60% of the maximum peak-to-peak force of the force generator, based on a previous study [4]. The loads transmitted to the small-scale airframe model from the linear force generator are measured using a force sensor (PCB 208C02, ③ in Fig. 13). Two single-axis accelerometers (PCB 352C42, ④ in Fig. 13) to measure the vertical airframe vibration responses are located, respectively, at the pilot and copilot seats of the manufactured small-scale model. An ICP sensor signal conditioner (PCB Model483C15, ⑤ in Fig. 13) is used for signal conditioning. MicrolabBox (⑥ in Fig. 13) acquires real-time

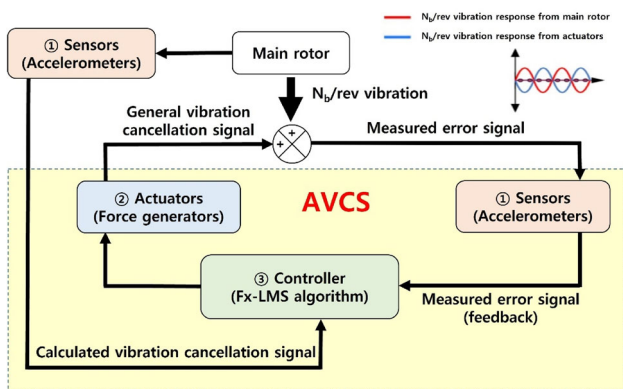**Table 7** Comparison of MAC values for small-scale models between analysis and test

Mode		Finite element analysis			
		1st lateral bending mode	1st vertical bending mode	2nd lateral bending mode	2nd vertical bending mode
Modal test	1st lateral bending mode	0.9261	0.8669	0.1426	0.1221
	1st vertical bending mode	0.8984	0.9029	0.1081	0.0914
	2nd lateral bending mode	0.0283	0.0093	0.8932	0.8816
	2nd vertical bending mode	0.0202	0.0043	0.8971	0.9030
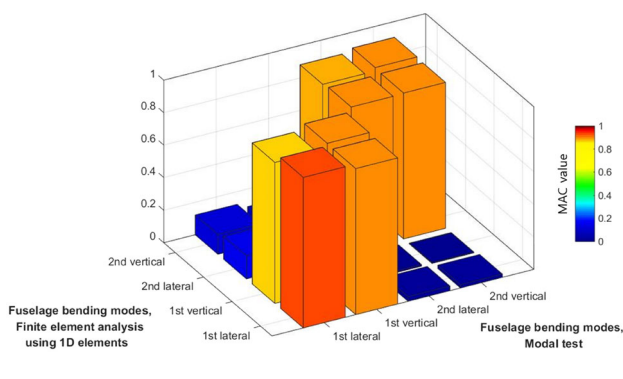
Fig. 9 3D presentation of MAC values for small-scale airframe models between analysis and test
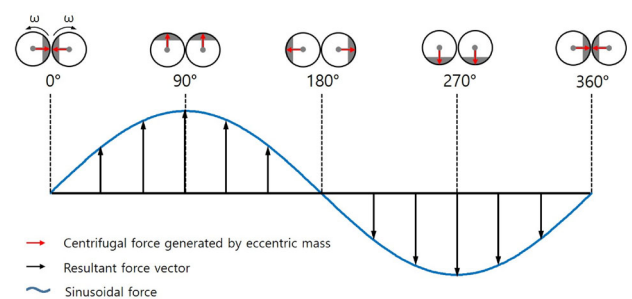
Fig. 11 Principle of producing linear force from counter-rotating force generator (CRFG)

Fig. 12 Schematic diagram of filtered-x least mean square (Fx-LMS) algorithm

2.4.2 AVCS Test Framework

Figure 15 shows the present AVCS test framework using Simulink blocks and dSPACE RTI Blockset in the MATLAB Simulink environment. The MATLAB Simulink file is connected to dSPACE ControlDesk. The excitation frequency is 4P for both a linear force generator for the hub vibratory pitch moment and two linear force generators for the vibration cancellation forces. The magnitudes of the forces for the hub pitch moment and the vibration cancellation are determined by system identifications for the disturbance path

Fig. 10 Schematic diagram of active vibration control system (AVCS) [17]

acceleration signals using the real-time interface (RTI) of MATLAB Simulink and delivers control signals to the linear force generators.
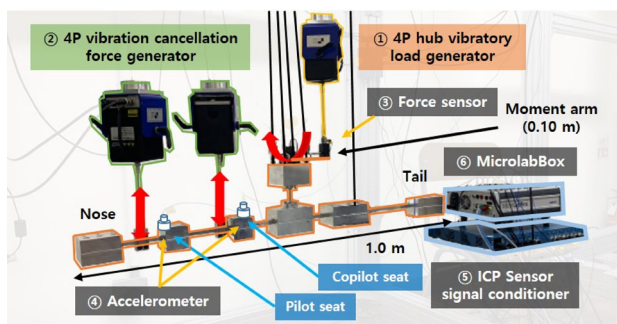
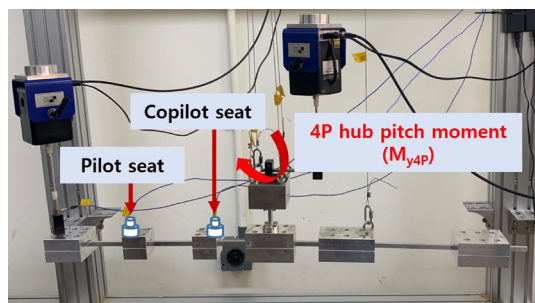**Fig. 13** Test bench setup using AVCS

Fig. 14 Measurement of airframe vibration responses of small-scale model

(H(iω), ① in Fig. 15a) and the actual forward path (C*(iω), ② in Fig. 15a) in Sect. 2.3. Figure 16 shows a schematic diagram of the signal acquisition and processing for the airframe vibration responses in the AVCS test using the manufactured small-scale GVT model. The control signals for the 4P hub pitch moment and vibration cancellation forces are input to the linear force generators (① and ② in Fig. 16) using the DAC channel of MicrolabBox (③ in Fig. 16). The acceleration data from the accelerometers (④ in Fig. 16) are delivered to the ADC channel. In addition, a band-pass filter (③ in Fig. 15b) is used to extract the airframe vibration responses with only the 4P frequency component.

2.5 AVCS Simulation Techniques

The AVCS simulation for the small-scale GVT model is conducted by constructing a framework based on MATLAB Simulink as shown in Fig. 17. The reference theta ($\theta(n)$, ① in Fig. 17) block represents the phase angle of the 4P hub pitch moment. The disturbance path (H(iω), ② in Fig. 17) block refers to the transfer function model obtained from the results of the vibration response analysis using the 4P hub pitch moment as the input value. The actual forward path (C*(iω), ③ in Fig. 17) block is the transfer function model defined using the airframe vibration responses when vibration cancellation forces are applied. With the update equation

(④ in Fig. 17) based on Fx-LMS algorithm, the control signal ($u(n)$) is updated to minimize the error signal, which is the sum of vibration cancellation signal ($\hat{y}(n)$) and airframe vibration response ($y(n)$) [17].

3 Results and Discussion

3.1 4P Airframe Vibration Responses at 250 Knots

Figure 18 shows the predicted and measured 4P vertical vibration responses from the test and simulation using the full- and small-scale GVT models at 250 knots when AVCS is not applied to the airframe model. Herein, to predict the 4P airframe vibration responses for the full-scale GVT model, 4P rotor hub vibratory loads (F_{x4P}, F_{z4P}, and M_{y4P}) at a flight speed of 250 knots from the previous study using CAMRAD II [21] are applied to the location of the rotor (node 25), using the same approach used in reference [17]. For the small-scale GVT model using 1D elements in both the test and simulation, the 4P hub pitch moment (M_{y4P}) only is applied to the rotor as previously described in Sect. 2.4.1. The magnitude of this 4P hub pitch moment is determined such that the 4P vertical airframe vibration responses of the small-scale GVT model in the test and simulation are similar to those of the full-scale GVT model and the prediction by Sikorsky [3]. As seen in the figure, at the pilot seat, the present simulations using the full- and small-scale GVT models compare well with the analysis by Sikorsky [3]. At the copilot seat, the present analyses using the full- and small-scale GVT models are lower than Sikorsky's result [3] by 14.78% and 28.12%, respectively; however, the measured result using the small-scale GVT model is correlated reasonably well with Sikorsky's analysis [3] because the relative difference is approximately 5.22%. Therefore, the present small-scale GVT model in both the test and simulation can appropriately represent the 4P X2TD airframe vibration responses in the vertical direction at 250 knots.

3.2 Correlation Between AVCS Test and Simulation

This section describes the correlation between the AVCS test and simulation results for the X2TD small-scale airframe model. However, the comparison between the results using the full- and small-scale models is not studied herein because the number and locations of force generators for AVCS are different in the two models. The acceleration data in the AVCS test are measured for 25 s, and AVCS is applied for 14 s from 6 to 20 s when the acceleration measurement is started. The value of the 4P airframe vibration responses reduced by AVCS are measured for 5 s from 15 s after the acceleration measurement begins to 20 s when the AVCS is terminated and the alleviated vibration is stabilized.

Fig. 15 Block diagrams of MATLAB Simulink for AVCS test
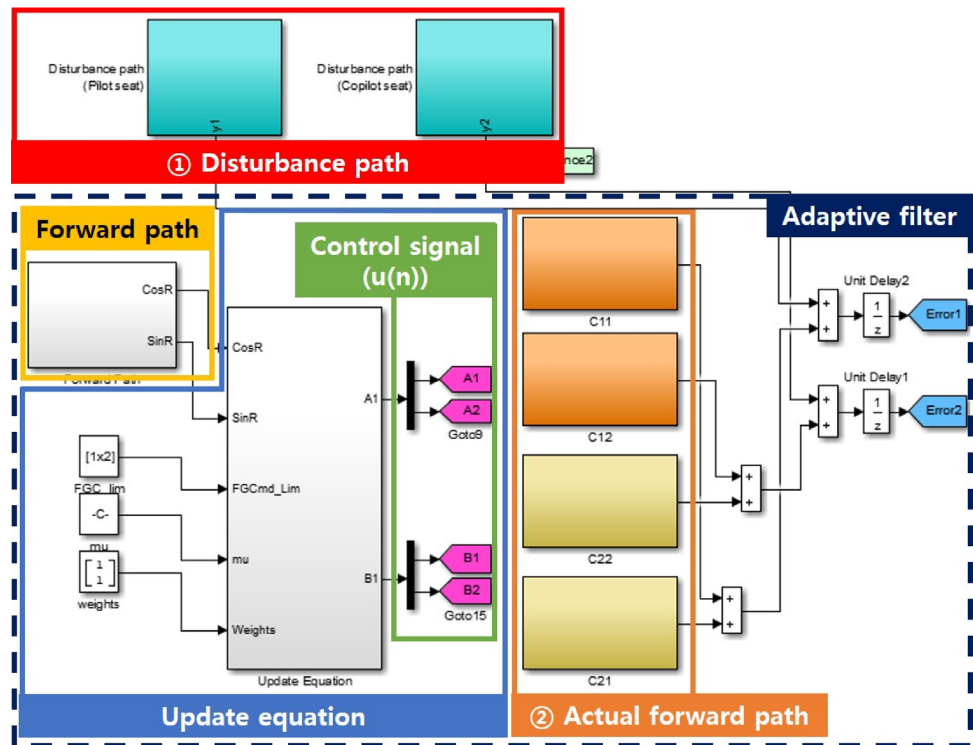
(a) AVCS using Fx-LMS algorithm in MATLAB Simulink environment
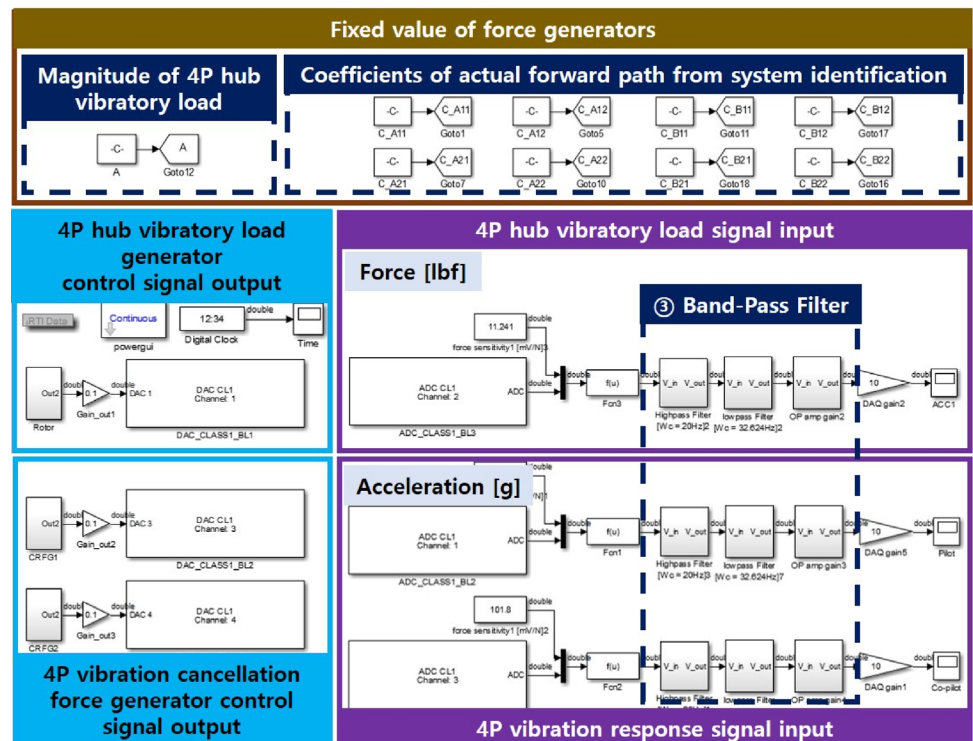
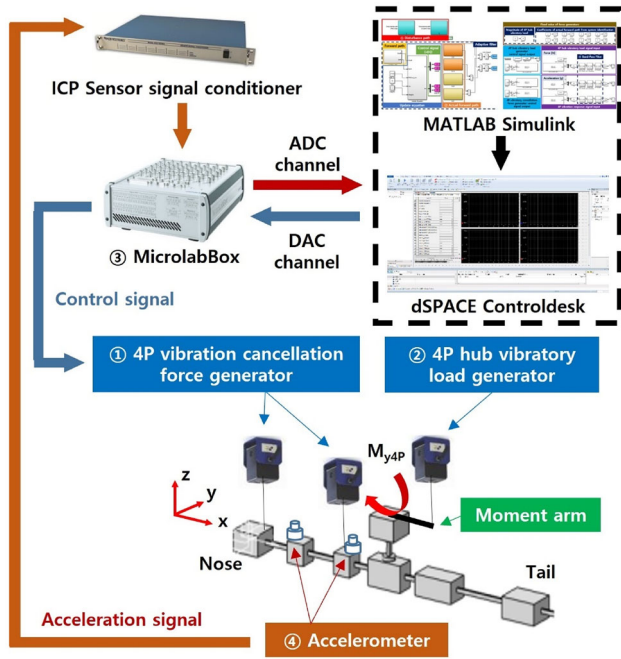(b) Signal input and output in real-time using dSPACE RTI

Fig. 16 Schematic diagram of AVCS test using small-scale airframe structure model

3.2.1 Multi-input–Single-Output Model

Prior to the study using AVCS with MIMO model, multi-input–single-output (MISO) model with two accelerometers and one force generator is considered for the AVCS. In this example, using the MISO model, the vibration reduction behaviors at the pilot and copilot seats are studied when the location of a force generator is changed. The MISO model
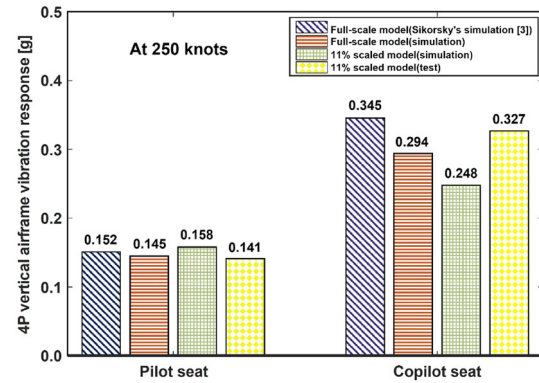

Fig. 18 Comparison of 4P vertical airframe vibration responses between full- and small-scale models

is obtained by modifying of the MIMO model discussed in Sect. 2.4. The 4P hub pitch moment only is used in this example, and its magnitude is determined such that the 4P vertical vibration responses at the pilot and copilot seats are similar to those of the full-scale model at 250 knots. The case study using AVCS in both the test and simulation is conducted with four cases, as shown in Fig. 19, when the four locations of a vibration cancellation force generator are considered. As the airframe vibration reductions at the pilot and copilot seats are mainly considered herein, there are four locations of a force generator near the pilot and copilot seats as shown in the figure. A vibration cancellation force generator in Case 1 is located ahead of the pilot seat; however, in Cases 2–4, it is placed between the pilot and copilot seats. Figure 20 shows the 4P vertical vibration responses at the pilot and copilot seats of the small-scale airframe model at 250 knots when
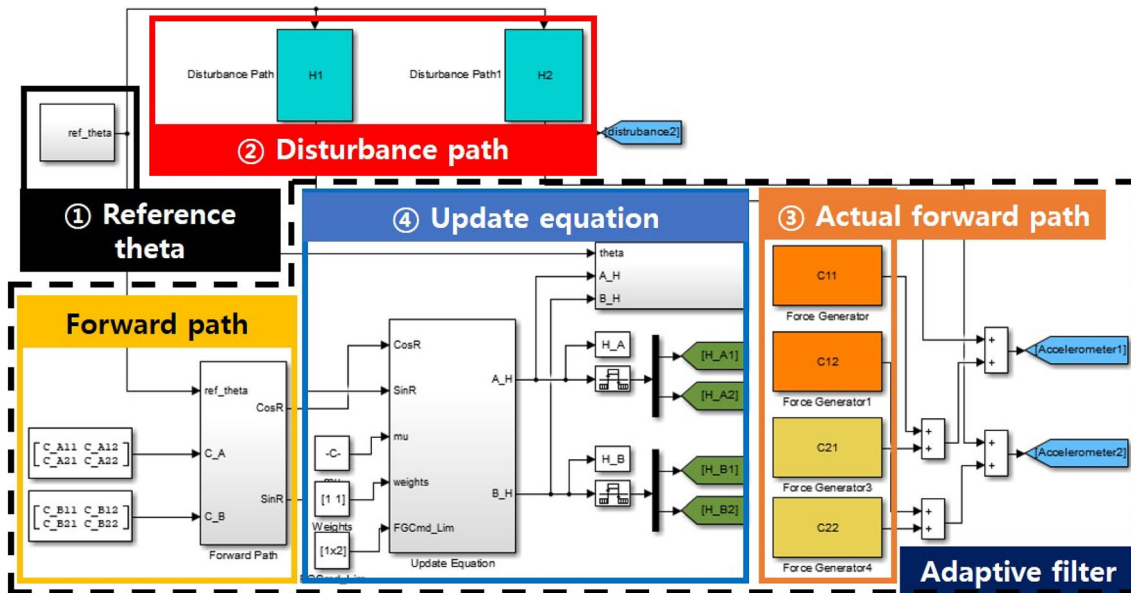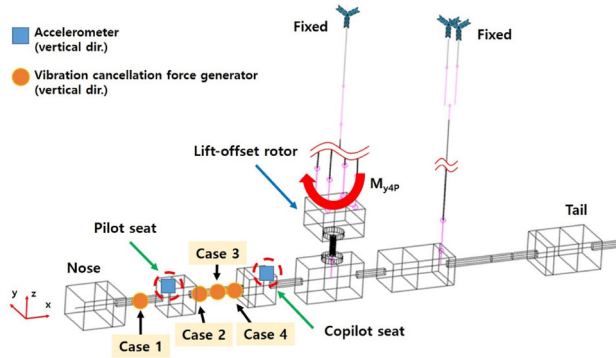

**Fig. 17** Block diagrams of MATLAB Simulink for AVCS simulation

Fig. 19 Locations of accelerometers and vibration cancellation force generators for MISO model

(a) Test

(b) Simulation

Fig. 20 4P vertical vibration reductions using AVCS with MISO model

the AVCS using the MISO model is applied in four cases. In the figure, the baseline indicates the 4P vertical vibration responses without AVCS. The relative error of the 4P vertical vibration responses without AVCS is 12.86 to 24.16% between the test and simulation in this example; therefore, its magnitude is moderate. However, the trend between the test and simulation is quite similar. The dashed lines show the trend of 4P vertical vibration reductions using different locations where the vibration cancellation force is applied. In the AVCS test, the reduced vibration response at the copilot seat gradually decreases from Cases 1 to 4, and a force generator is located from far to near the copilot seat. This trend is similar to that observed in the simulation. At the pilot seat in Case 1 in which a force generator placed near the pilot seat, the vibration reduction is higher than that of the other cases. The vibration responses at the pilot seat obtained from Cases 1 to 4, wherein the distance between the force generator's location and the pilot seat is from short to long in the test, also show a similar trend to the simulation. Although the results for all four cases show relative errors of 9.76 to 38.86% between the AVCS test and simulation, this error is appropriate because the error magnitude is acceptable compared with the error of 68% in reference [4]. Based on the results obtained using the MISO model in this section, the two vibration cancellation force generators are located near the pilot and copilot seats to reduce the 4P vertical vibration responses at the pilot and copilot seats effectively in the next section using the MIMO model.

3.2.2 Multi-input–Multi-output Model

A correlation study for the AVCS test and simulation using a small-scale airframe structure with the MIMO model is conducted using the techniques described in Sect. 2.4. When comparing the AVCS test results with the simulation results, the 4P vertical vibration response behaviors in the time domain, required time for convergence of the vibration response reduced by AVCS, and vibration reduction rate are
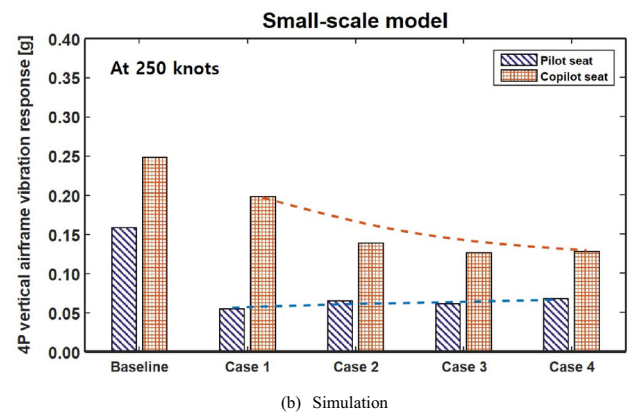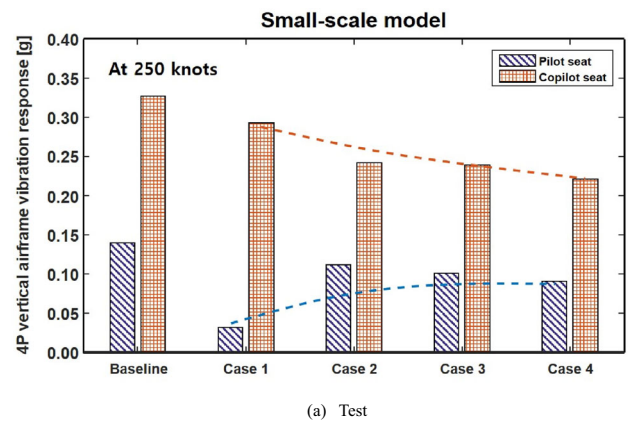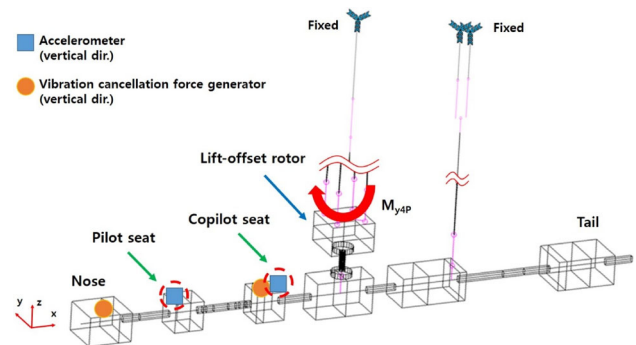

Fig. 21 Locations of accelerometers and vibration cancellation force generators for MIMO model

considered. A 4P hub pitch moment with the same magnitude as that used for the previous example with the MISO model is applied in this section. The locations of the two vibration cancellation force generators and accelerometers at the pilot and copilot seats are shown in Fig. 21. The locations of the two vibration cancellation force generators are determined to obtain excellent vibration reduction performance based on previous results using the MISO model. Figures 22 and 23 show the 4P vertical vibration responses reduced using the AVCS at the pilot and copilot seats, respectively, in the time domain. In the test, the 4P vertical vibration response
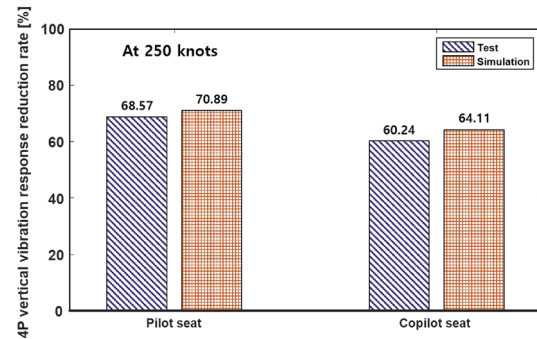
(a) Test

(b) Simulation
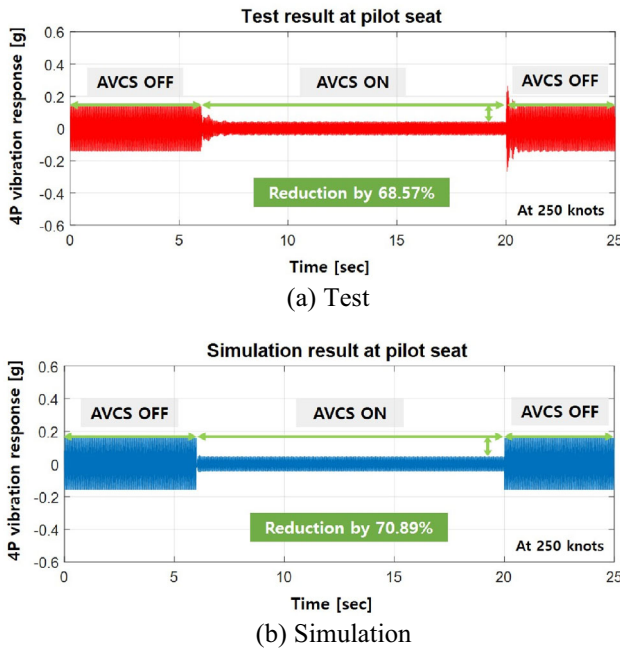
Fig. 22 Reduced 4P vertical vibration responses using AVCS at pilot seat of small-scale model

(a) Test

(b) Simulation

Fig. 23 Reduced 4P vertical vibration responses using AVCS at copilot seat of small-scale model

at the pilot seat reduced by AVCS (0.044 g) is less than the target level of the X2TD airframe vibration (0.1 g, [3]) and the reduced vertical vibration response at the copilot seat is measured as 0.130 g, which is similar to the target value of 0.1 g. In addition, the reduced vertical vibration responses at the pilot and copilot seats in the simulation have magnitudes of 0.046 g and 0.089 g, respectively, both of which are lower than 0.1 g. Hence, the vibration reduction performance using AVCS is good in both the test and simulation herein. The differences in the reduced vibration responses between the test and simulation when AVCS with the MIMO model is applied are 4.55% and 31.54% at the pilot and copilot seats, respectively. The differences are less than the value given in reference (68%, [4]); thus, the differences between the AVCS test and simulation are reasonable and acceptable in this study. In addition, the measured 4P vertical vibration response behaviors in the time domain are similar to the predicted results, as shown in the figures, and the 4P vertical vibration responses at both the pilot and copilot seats converge within 2 s after AVCS is applied in both the test and simulation. However, as shown in Fig. 22a, when AVCS is applied, the 4P vertical vibration response does not immediately converge to the reduced vibration response (0.044 g) owing to the reaction to the oscillation of springs with low stiffness in the GVT model. The reduction rates of the 4P vibration responses at the pilot and copilot seats in the test and simulation are summarized in Fig. 24. As seen in the figure, the vibration reduction rates in the AVCS test are 68.57% and 60.24% at the pilot and copilot seats, respectively, and the simulation results are 70.89% and 64.11%, respectively.
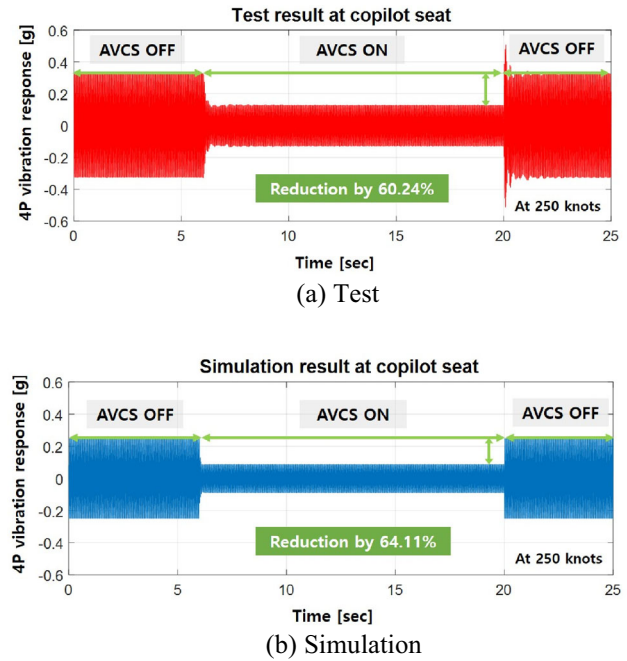
Fig. 24 4P vertical vibration response reduction rates for small-scale model using AVCS

Therefore, there are small errors of −2.32% and −3.87% at the pilot and copilot seats, respectively, when the AVCS test results are compared with the simulation results. Finally, it can be concluded that the present AVCS test and simulation results are reasonably similar, and the vibration reduction capability using AVCS with the MIMO model is excellent for the X2TD small-scale airframe model.

4 Conclusion

In this study, the active airframe vibration control test and simulation studies using AVCS were conducted for a Sikorsky X2TD lift-offset compound helicopter at a flight speed of 250 knots. The 11% scaled airframe structure was designed and manufactured such that the dynamic similarity between the full-scale X2TD airframe model and the present small-scale model was satisfied. The 4P hub pitch moment only

was applied to the small-scale GVT model, such that its 4P vertical vibration responses at the pilot and copilot seats were similar to those of the full-scale airframe model at 250 knots. In this AVCS study, two linear force generators were used to produce vibration cancellation forces in the vertical direction. The vibration cancellation forces were determined using the Fx-LMS algorithm, which is a closed-loop feedback controller. The single-axis accelerometers were located at the pilot and copilot seats to measure the vertical vibration responses; however, MSC.NASTRAN was used to predict the vertical vibration responses of the small-scale GVT model in the AVCS simulation. The AVCS framework in both the test and simulation was constructed using MATLAB Simulink, and dSPACE MicrolabBox equipment was applied in the AVCS test.

First, when AVCS using the MISO model with one force generator and two accelerometers was applied for four case studies, it was investigated that the force generators were required to be located near the pilot and copilot seats for good vibration reduction at the pilot and copilot seats. The 4P vertical vibration reductions in the AVCS test were compared with the simulation results, and the differences between the two results were 9.76–38.86% for the four cases. Second, an AVCS study was conducted with a MIMO model using two force generators and two accelerometers. The 4P vertical vibration responses in the AVCS test were reduced by 68.57% and 60.24% from the baseline without AVCS, respectively, at the pilot and copilot seats, and the vibration reduction rates in the AVCS simulation were 70.89% and 64.11%, respectively. The relative errors between the AVCS test and simulation were -2.32% and -3.87% at the pilot and copilot seats, respectively. Therefore, this study showed that the AVCS test and simulation results were similar for the X2TD small-scale airframe model at 250 knots, and the 4P vertical vibration reductions using AVCS were good at the pilot and copilot seats.

Declarations

Conflict of Interest The authors declare that there is no conflict of interest regarding the publication of this paper.

References

1. Ruddell AJ (1981) Advancing blade concept (ABC) technology demonstrator. USAAVRADCOM-TR-81-D-5
2. Bagai A (2008) Aerodynamic design of the X2 technology demonstrator[TM] main rotor blades. In: Proceedings of 64th American Helicopter Society Annual Forum
3. Blackwell R, Millott T (2008) Dynamics design characteristics of the sikorsky X2 Technology[TM] demonstrator aircraft. In: Proceedings of 64th American Helicopter Society Annual Forum
4. Kim D-H, Kim T-J, Jung S-U, Kwak D-I (2016) Test and simulation of an active vibration control system for helicopter applications. Int J Aeronaut Space Sci 17(3):442–453
5. Kim D-H, Kwak D-I, Song Q (2019) Demonstration of active vibration control system on a Korean utility helicopter. Int J Aeronaut Space Sci 20(1):249–259
6. Kim D-H (2021) Multicyclic helicopter vibration control. Trans Korean Soc Noise Vib Eng 31(3):247–259
7. Lee Y-L, Kim D-H, Park J-S, Hong S-B (2020) Vibration reduction simulations of a lift-offset compound helicopter using two active control techniques. Aerosp Sci Technol 106:106181
8. Kvaternik RG, Juang J-N, Bennett RL (2000) Exploratory studies in generalized predictive control for active aeroelastic control of tiltrotor aircraft," NASA TM2000 210552
9. Rangacharyulu MA, Moore MJ (1991) Flight vibration testing of the V-22 tiltrotor aircraft. In: Proceedings of 47th Annual Forum of the American Helicopter Society
10. Hong S-B, Park J-S (2021) Active vibration control test of high-speed compound unmanned rotorcraft using scaled airframe model. Trans Korean Soc Noise Vib Eng 31(6):642–653
11. Elliot SJ, Nelson PA (1993) Active noise control. In: IEEE signal processing magazine, pp. 12–35
12. Kwon Y-M, Hong S-B, Lee Y-B, Park J-S (2022) Active vibration reductions of a lift-offset compound helicopter using individual blade pitch control with multiple harmonic inputs. Aircr Eng Aerosp Technol 94(6):994–1008
13. Dompka RV (1989) Investigation of difficult component effects on finite element model vibration prediction for the bell AH-1G helicopter," NASA CR 181916
14. Abhishek A, Chopra I, Purekar A, Wang G, Phan N, Semidey R, Leibshutz D (2012) Rotor load prediction using coupled rotor/fuselage model and sensor data. In: Proceedings of 68th American Helicopter Society Annual Forum
15. Degener M, Hermes M (1996) Ground vibration test and finite element analysis of the GARTEUR SM-AG19 Testbed. DLR Report IB 232-96 J08
16. Johnson W, Moodie AM, Yeo H (2012) Design and performance of lift-offset rotorcraft for short-haul missions. In: Proceedings of American Helicopter Society Future Vertical Lift Aircraft Design Conference
17. Hong S-B, Kwon Y-M, Kim J-S, Lee Y-B, Park B-H, Shin H-C, Park J-S (2021) Active airframe vibration control simulations of lift-offset compound helicopters in high-speed flights. J Korea Inst Milit Sci Technol 24(4):357–367
18. Pastor M, Binda M, Harčarik T (2012) Modal assurance criterion. Proc Eng 48:543–548
19. Kim D-H (2017) Accelerometer signal processing for a helicopter active vibration control system. J Korean Soc Aeronaut Space Sci 45:863–871
20. Kim J-S, Hong S-B, Kwon Y-M, Park J-S (2021) Effect of lift-offset rotor hub vibratory load components on airframe vibration responses of high-speed compound unmanned rotorcrafts. J Korea Inst Milit Sci Technol 24(3):255–263
21. Kwon Y-M, Park J-S, Wie S-Y, Kang HJ, Kim D-H (2021) Aeromechanics analyses of a modern lift-offset coaxial rotor in high-speed forward flight. Int J Aeronaut Space Sci 22(2):338–351